Temporal changes of event size distribution during episodes of shallow tectonic tremor, Nankai trough

Masaru Nakano[1] and Suguru Yabe[2]

[1]Research Institute for Marine Geodynamics, Japan Agency for Marine-Earth Science and Technology, 2-15, Natsushima-cho, Yokosuka-City, Kanagawa 237-0061, Japan

[2]Geological Survey of Japan, National Institute of Advanced Industrial Science and Technology (AIST), Tsukuba Central 7, 1-1-1 Higashi, Tsukuba, Ibaraki 305-8567, Japan

Corresponding author: Masaru Nakano (mnakano@jamstec.go.jp)

Key Points:

- The slope and cut-off magnitude of event size distribution changed during episodes of shallow tectonic tremor along the Nankai trough
- The 2D PCA slow earthquake model can explain these changes by changes in event ignition probability or energy dissipation during slip
- Observed changes imply release of accumulated stress or decrease of pore fluid pressure on the fault interface during each tremor episode

Abstract

Slow earthquakes follow a power-law size distribution with an exponential taper for the largest events. We investigated changes in the size distribution of shallow tectonic tremor events during two prolonged tremor episodes (>1 month) along the Nankai trough and found that the slope of the size distributions increased while the cut-off magnitudes decreased late during each episode, as tremor activity waned. Interpreting these changes with the two-dimensional probabilistic cell automaton model of slow earthquakes, we found that a decrease in event ignition probability or an increase in energy dissipation during slip can qualitatively explain the observed changes. These changes imply that a decrease in accumulated stress or pore-fluid pressure on the fault interface occurred during each tremor episode. Because the tremor source migrates during an episode, the changes in the size distribution parameters can be attributed to spatial variations or temporal changes in the source characteristics.

Plain Language Summary

The size distribution of slow earthquakes mostly follows a power law like that of ordinary earthquakes, in which the logarithm of event numbers is negatively proportional to the logarithm of event sizes, with an exponential taper for events larger than a cut-off magnitude. We investigated the changes in this size distribution during two prolonged episodes of shallow tectonic tremor that occurred on the plate interface along the Nankai trough, southwestern Japan. We found that the ratio of smaller events increased and the cut-off magnitude decreased as tremor activity decreased late in each episode. We interpreted this observation by using a model of slow earthquakes that divides a source fault into small cells and updates slip on each cell probabilistically. The model can explain the changes in the tremor size distribution by a decrease in the probability of event ignition or an increase in the energy dissipation during fault slip. This result implies that the accumulated stress or the pore-fluid pressure on the source fault decreased when the tremor was less active. Because the tremor source migrates during the course of each episode, these changes indicate that the source characteristics of tremor vary at different times or locations.

1 Introduction

Slow earthquakes, fault slips with longer durations than ordinary earthquakes of similar magnitudes, mostly occur in areas surrounding the source regions of megathrust earthquakes in subduction zones (e.g., Obara & Kato, 2016). Signals of a slow earthquake may be termed as tectonic tremor, a very low frequency earthquake (VLFE), or a slow slip event (SSE) depending on the frequency band of the observations, all of which share common fault slips because they occur concurrently in the same source region (e.g., Araki et al., 2017; Ito et al., 2007; Kaneko et al., 2018; Obara & Hirose, 2006; Obara et al., 2004; Rogers & Dragert, 2003). The source process of slow earthquakes is studied through the analysis of scaling relationships among the source characteristics: event duration, recurrence interval, size of the source fault, seismic moment release, radiated seismic energy, and so on (e.g., Ide & Yabe, 2014; Ide et al., 2007; Tan & Marson, 2020; Yabe et al., 2019). Recent studies suggest that heterogeneities in the frictional properties on the fault control the distribution of events and their source characteristics (e.g., Baba et al., 2020; Nishikawa et al., 2019; Obara et al., 2010; Takemura et al., 2019; Tanaka et al., 2019).

The event size distribution is one of the scaling relationships that characterize the source processes of seismic phenomena. Ordinary earthquakes follow the Ishimoto-Iida or Gutenberg-Richter (GR) law (e.g., Gutenberg & Richter, 1944; Ishimoto & Iida, 1939), a power-law relationship implying that the source fault is self-similar. The negative of the slope (the b-value) is commonly related to the stress state of the medium (Scholz, 1968, 2015). In contrast, volcanic tremor follow exponential-law size distributions (e.g., Benoit & McNutt, 2003), implying that the source process has a characteristic size. Most studies have shown that slow earthquakes follow a power-law size distribution (Bostock et al., 2015; Ito et al., 2009; Kao et al., 2010; Nakamura & Sunagawa, 2015; Staudenmaier et al., 2019; Wech et al., 2010), although some observations indicate that they follow an exponential-law size distribution (Chestler & Creager, 2017; Yabe & Ide, 2014).

A recent study of shallow tectonic tremor along the Nankai trough (Nakano et al., 2019) found that the event size distribution follows a tapered Gutenberg-Richter (TGR) distribution (Kagan, 2002), given by

$$\Phi(M) = (M_\mathrm{t}/M)^{\beta} \exp\left(\frac{M_\mathrm{t}-M}{M_\mathrm{c}}\right) \qquad \text{for} \quad M_\mathrm{t} < M < \infty, \qquad (1)$$

where M is seismic moment, M_t is the catalog completeness threshold, and M_c is the corner moment. β controls the slope of the distribution; $\beta = 2b/3$ in the ordinary Gutenberg-Richter law. A TGR distribution may reconcile the contradictory findings of previous studies: power-law distributions better fit the overall size distribution, but exponential distributions may better fit the observations when only the largest events are observable. For ordinary earthquakes, the b-value of the GR law, and accordingly β, has been related to the stress level in the medium (Scholz, 1968, 2015), and the corner moment M_c may be related to the fault dimension, which is specific to the causative fault (Kagan, 2002). For Nankai trough slow earthquakes, both β and M_c differ during different time periods in the same source region (Nakano et al., 2019), implying that the source characteristics of these events change with time, although the cause is poorly understood.

In this study, we analyzed the size distributions of shallow tectonic tremor along the Nankai trough during tremor episodes that occurred off the city of Kumano, Mie Prefecture, in 2016 and off the Kii Channel in 2018. By fitting the data with the TGR distribution, we found that the size distribution parameters of shallow tectonic tremor changed during the course of each episode, indicating that the source characteristics changed. We qualitatively interpreted the controlling factors of this distribution using the probabilistic cell automaton (PCA) model for slow earthquakes proposed by Ide and Yabe (2019). We found that the changes in the tremor event size distributions can be attributed to changes in the accumulated stress or the pore pressure on the fault.

2 Observed changes of tremor size distributions

2.1 Estimation of tremor size distribution

Using data obtained from the permanent Dense Oceanfloor Network System for Earthquakes and Tsunamis (DONET; Kaneda et al., 2015; Kawaguchi et al., 2015; Figure 1), we analyzed intensive tremor episodes with durations longer than a month; these include one that occurred off Kumano in April 2016, with a duration of about a month, and another off the Kii

Channel that started in mid-February 2018 and continued for about 4 months (Figure 1). We referred to the seismic energy catalog of Nakano et al. (2019) for the 2016 off-Kumano activity, and for this study we estimated the radiated seismic energy of tremor events during the 2018 off-Kii Channel activity.

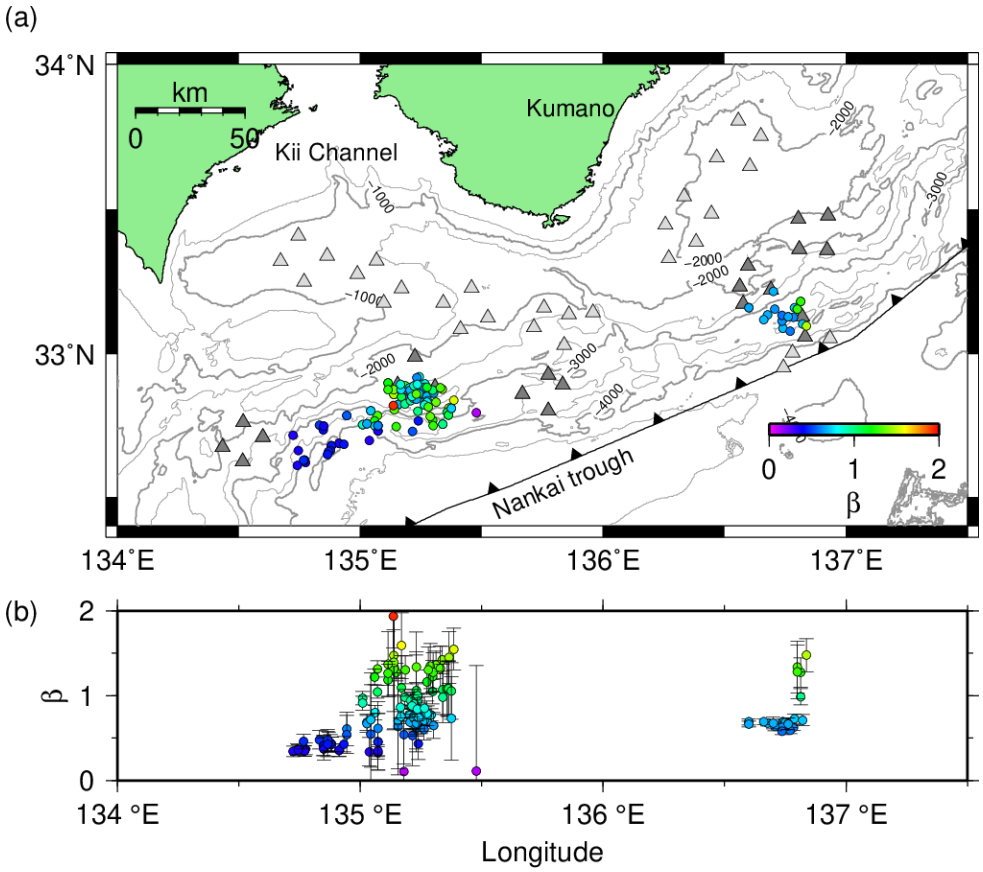

Figure 1. (a) Map showing locations of DONET stations (triangles) and 10-day average locations of tectonic tremor events (circles). Dark gray triangles indicate DONET stations used in this study. Colors of circles represent the slope (β) of the size distribution of tremor events (10-day averages). (b) Longitudinal distribution of β. Error bars indicate the standard error of β values.

We estimated tremor energy by the method of Nakano et al. (2019). We first determined tremor source locations by the envelope correlation method (Ide, 2010; Obara, 2002). We used the daily average of these locations (Figure S1) for energy estimations because of their large scatter, which may be due to strong heterogeneities in velocity structures in the accretionary prism (Takemura et al., 2020). We next computed the energy rate waveforms at the source from three-component seismograms that were band-pass filtered between 2 and 8 Hz and corrected for the site amplification factors given by Yabe et al. (2020). We defined a tremor event as one in which the seismic energy rate continuously exceeded a threshold of 10^2 J/s. Nakano et al. (2019) tried thresholds ranging between 10 and 10^3 J/s and found that they do not affect the nature of the size distributions. The seismic energy of each tremor event was then obtained by integrating the energy rate waveform over the time during each event. As the seismic energy of the tremor

signal is proportional to the seismic moment (Ide & Yabe, 2014; Yabe et al., 2019), we used these seismic energy estimates to represent the tremor event size. Signals from ordinary earthquakes were removed by reference to the catalogs of the Japan Meteorological Agency and U.S. Geological Survey.

To investigate the changes in event size distributions during each tremor episode, we fitted the TGR distribution given by equation (1) to the size distributions obtained from sliding 10-day time windows (Figure 2). We assumed a catalog completeness magnitude M_t of 3.0×10^4 J.

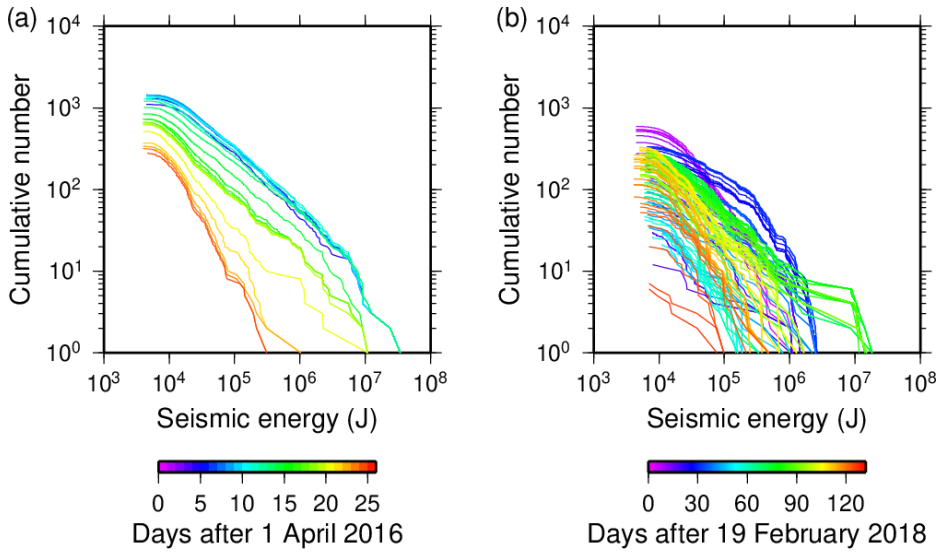

Figure 2. Size distributions of tectonic tremor during successive 10-day sliding time windows for (a) the 2016 off-Kumano episode and (b) the 2018 off-Kii Channel episode.

2.2 Changes of tremor size distributions

Figure 3 shows how the size-distribution parameters β and M_c of the TGR distribution changed with time for the 2016 off-Kumano and 2018 off-Kii Channel tremor episodes; β increased and M_c decreased near the end of the 2016 episode and in the middle and end of the 2018 episode. The change was also clear in the event size distributions of successive 10-day time windows (Figure 2). Because the tremor source migrated during each episode (Figure S1), we plotted the distributions of β and M_c in Figures 1 and S2, respectively, at positions representing the 10-day average of tremor source locations. In the 2016 off-Kumano episode, higher β values with lower M_c were concentrated at the southeast end of the source area. In the 2018 off-Kii Channel episode, the activity was mainly concentrated between longitude 135.0°E and 135.5°E, and both β and M_c showed distinct variations in this area. We note that these estimations were from tremor events scattered within 10–20 km of the average location. These results imply that the changes in the size-distribution parameters may be caused by spatial or temporal changes in the source characteristics of the tremor events.

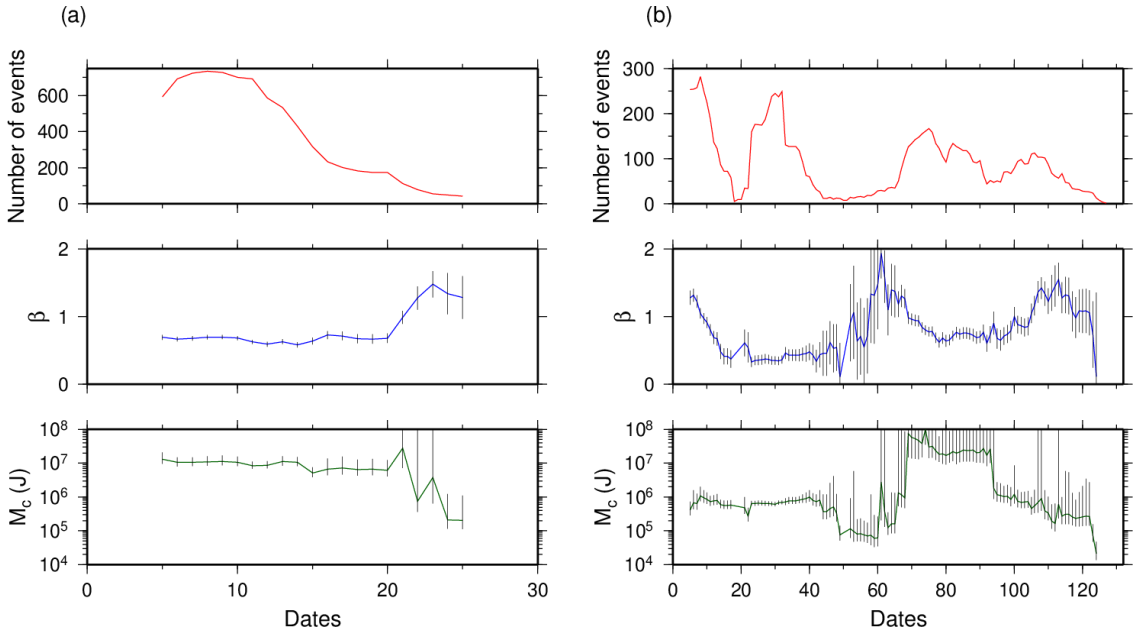

Figure 3. Temporal changes of event number and the slope β and corner moment M_c of the tremor size distributions obtained from 10-day sliding time windows during the (a) 2016 off-Kumano and (b) 2018 off-Kii Channel episodes. Vertical bars represent uncertainties on β and M_c.

3 Size distribution of slow earthquakes expected from the 2D PCA model

3.1 2D PCA model

We investigated the cause of the observed changes in the tremor event size distributions by using the 2D PCA model of slow earthquakes proposed by Ide and Yabe (2019), which is an extension of the 1D Brownian slow earthquake model (Ide, 2008) to a 2D source fault. This model has successfully reproduced various scaling relationships of slow earthquakes, including their TGR-like event size distributions. In the 2D PCA model, the fault plane of a slow earthquake is divided into $N_x \times N_y$ cells, and each cell has two states: "stop" and "slip". The state of each cell is updated stochastically according to the states of neighboring cells: Each "stop" cell becomes a "slip" cell with a probability $N_b p_b$, where N_b is the number of surrounding cells in the "slip" state and p_b is a probability of interactions between adjacent cells, and each "slip" cell becomes a "stop" cell with a probability $(4 - N_b)p_b$. In addition, Ide & Yabe (2019) introduced the random ignition of slip in a cell with a probability p_l, which may be related to the slow loading from the surrounding medium. They also considered energy dissipation during slip, which suppresses slip in the cell with a probability p_v, introducing an additional characteristic scale to the event size distribution. The status of each cell (v_i^k) is updated based on

$$v_i^{k+1} = H\left(v_i^k + p_b \sum_{NN}\left(v_j^k - v_i^k\right) + p_l - p_v v_i^k - \xi\right), \quad (2)$$

where NN represents the four nearest neighbor cells, $H()$ is the Heaviside function, i and k represent the cell number and time step, respectively, and ξ is a random number with a

uniform distribution between 0 and 1 (Ide & Yabe, 2019). The value of v_i^k is 0 in the "stop" state and 1 in the "slip" state.

3.2 Dependence of tremor size distribution on probability parameters

We used the 2D PCA model to investigate the dependence of β and M_c for the tremor size distribution on each of the probability parameters for synthetic tremor. We simulated tremor events with a fixed source size $N_x = N_y = 101$ for 10^6 steps. The tremor event size was defined as the total number of slipped cells during a tremor event, which ends when the number of slipping cells becomes zero. The dependence on p_b was surveyed for tremor events computed with $p_l = p_v = 0.0$. The dependences on p_v and p_l were studied for fixed values of $p_l = 0.0$ and $p_v = 0.01$, respectively, with $p_b = 0.1$. We note here that p_l should be smaller than p_v, otherwise the slipping cells proliferate without suppression (see equation 2). Then we estimated the size-distribution parameters β and M_c by fitting the TGR distribution to the event size distributions synthesized by using each combination of the probability parameters by setting $M_t = 100$ event size units. The event size distributions of the synthetic tremor computed by varying p_b, p_l, and p_v are shown in Figures S3, S4, and S5, respectively.

Figure 4 shows the dependence of β and M_c values for each probability parameter of the 2D PCA model. When the ignition probability p_l increases, the slope β of the size distribution decreases while the corner event size M_c increases. The anti-correlation of p_l and β is similar to the known anti-correlation between the b-value of the GR law and the stress level in the medium for regular earthquakes (Scholz, 1968, 2015). The dependence on the stopping probability p_v was opposite to the dependence on p_l. This behavior is easily understood because these probability parameters have opposite signs in equation (2). Energy dissipation during slip suppresses growth of the event, and accordingly the ratio of large events to small events decreases. This effect introduces an additional characteristic size to the system and accordingly reduces M_c. The dependence on the probability p_b is rather complex. Both β and M_c increase as p_b increases for $p_b < 10^{-2}$, whereas M_c decreases while β remains almost constant for $p_b > 10^{-2}$. When p_b is too small, slip on a cell hardly propagates to surrounding cells and a slipping cell hardly stops, in which case the event size is mostly determined by the duration of slip at one cell. We do not expect such behavior for the source of short-term slow earthquake episodes. When p_b is large enough, slip on a cell easily propagates to surrounding cells and slip in a cell easily stops when it is surrounded by "stop" cells, which may reduce event durations and decrease M_c at the largest p_b values.

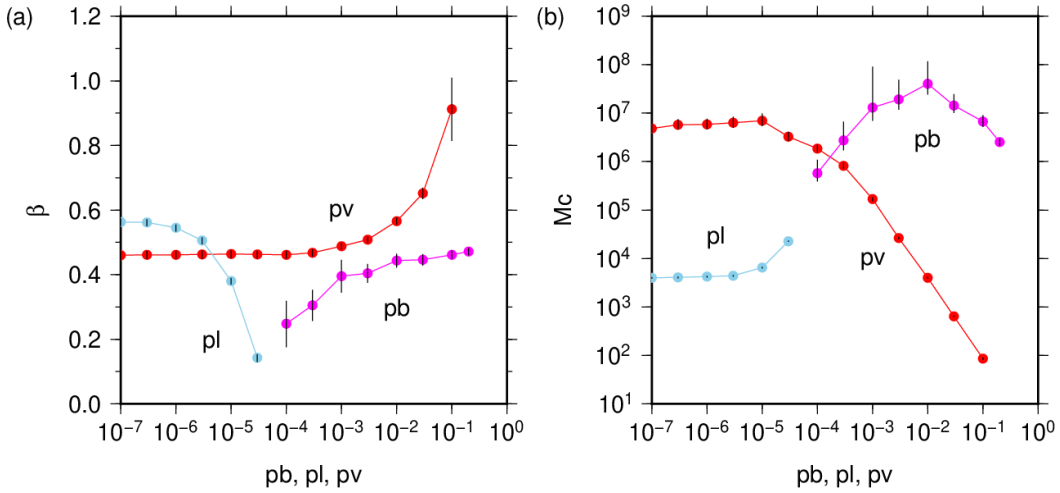

Figure 4. Dependence of the size distribution parameters β and M_c of synthetic tremor activities on three probability parameters (p_b, p_l, and p_v) computed from the 2D PCA model (Ide & Yabe, 2019). See section 3 in the text for explanation.

4 Discussion

In both of the tremor episodes we studied along the Nankai trough, β increased as M_c decreased in the later part of the episode as the rate of events decreased. These changes can be qualitatively explained in the 2D PCA model by a decrease in the event ignition probability p_l or an increase in the energy dissipation probability p_v. In the following, we discuss the causes that may change these probabilistic parameters during slow earthquakes. Because the tremor sources migrated during each episode (Figure S1), the changes in these parameters may represent spatial or temporal changes in the source characteristics.

The main factors that control slow earthquake activity are the stiffness of the host rock, stress accumulation, and frictional resistance on the fault interface. Host rock stiffness may control the interactions of fault slip with the local surroundings, which was modeled as the probability p_b in the 2D PCA model, but cannot explain the observed changes of the tremor size distributions.

Accumulated stress on the causative fault drives the spontaneous activity of regular and slow earthquakes (e.g., Matsuzawa et al., 2010). Accumulated stress that is initially high is released gradually in slow earthquakes. This change may decrease the event ignition probability p_l that is consistent with the observed β increase and M_c decrease in the later part of tremor episodes. Because the slip history of previous slow earthquakes may result in a heterogeneous distribution of accumulated stress (e.g., Matsuzawa et al., 2010), the migration of tremor sources may also affect the tremor size distributions. It is challenging to estimate the stress accumulation on a source fault before an event occurs; however, the degree of coupling between the overriding and subducting plate may affect the stress accumulation rate and accordingly the slip ignition probability. The coupling ratio on the plate interface has been found to be spatially heterogeneous along the Nankai trough (Nishimura et al., 2018; Noda et al., 2018; Yokota et al., 2016) and is inversely correlated with slow earthquake activity (Baba et al., 2020; Takemura et

al., 2019). Hence, spatial variations of the coupling ratio may also be related to event size distributions.

Frictional resistance depends on the pore-fluid pressure on the fault interface. Because an increase in pore-fluid pressure reduces the normal stress and accordingly the frictional resistance, pore fluid is considered a primary trigger of slow earthquakes (e.g., Kato et al., 2010; Obara, 2002). Theoretical studies modeling slow earthquakes have assumed that pore fluid reduces the normal stress on the fault (e.g., Gao & Wang, 2017; Liu & Rice, 2007; Matsuzawa et al., 2010). A decrease in pore-fluid pressure increases frictional resistance during slip and therefore increases the energy dissipation probability p_v or decreases the slip ignition probability p_l in the 2D PCA model. The observed β increase and M_c decrease can be explained by a decrease of pore-fluid pressure as tremor activity decreases in the later part of tremor episodes.

The excess pore-fluid pressure inferred from low shear-wave velocity anomalies in the accretionary prism has been correlated with the distribution of shallow VLFEs along the Nankai trough (Kitajima & Saffer, 2012; Tonegawa et al., 2017). Recent studies have detected along-dip and along-strike variations of tremor and VLFE activities, implying that heterogeneous frictional properties on the plate interface affect slow earthquake activity (Nishikawa et al., 2019; Tanaka et al., 2019; Yabe et al., 2019, 2020). The heterogeneous distribution of pore-fluid pressure and frictional properties on the fault interface may change the event size distribution of tremor as it migrates. At shallow depths, the frictional properties of clay gouge produce velocity-strengthening behavior when water is included in minerals' interlayers (Ikari et al., 2007). Clay minerals become dehydrated at depths greater than 8 km by the increased temperature and pressure, and the resulting fluid may exist in pore spaces rather than in the clay minerals (Ikari et al., 2007). The dehydration depth is close to the source depths of VLFEs along the Nankai trough (Nakano et al., 2018; Sugioka et al., 2012). Since VLFEs and tectonic tremor are the same phenomena but observed in different frequency ranges (Kaneko et al., 2018; Masuda et al., 2020), depth-dependent frictional properties may also affect the event size distribution of tectonic tremor.

Seismic observations have detected migrations of pore fluid coincident with slow earthquakes (Gosselin et al., 2020; Kano et al., 2019; Nakajima & Uchida, 2018; Warren-Smith et al., 2019; Zal et al., 2020), implying that pore-fluid pressure on the fault changes during a tremor episode. Tidal stress changes also affect normal stress and thereby tremor activity (e.g., Ide & Tanaka, 2014), but we can ignore this effect because the changes we detected in size distribution parameters occurred in time windows 10 days long.

In this study, we interpreted observed changes in the size distributions of tectonic tremor based on the 2D PCA model. The slope β expected from the 2D PCA model is usually 0.5, a value that is smaller than the observed values except for the largest p_v values. Although the 2D PCA model reproduces certain statistical characteristics of slow earthquakes, such as duration-moment scaling and TGR size distribution, there remains room for improvement. For example, the 2D PCA model only considers interactions with the nearest neighboring cells and ignores interactions with more distant cells. It also does not include the effects of slip history, which are necessary to reproduce lateral migrations over long distances. Therefore, the interpretations in this study are still qualitative. Further improvement of data analysis and theoretical models is needed to improve our understanding of the source process of slow earthquakes.

5 Conclusions

Shallow tectonic tremor along the Nankai trough follow the tapered Gutenberg-Richter distribution (Kagan, 2002), a power-law distribution of event sizes with an exponential taper for the largest events. In our study of temporal changes of the event size distribution of shallow tectonic tremor during long tremor episodes off Kumano in 2016 and off the Kii Channel in 2018, we found that the slope of the event size distribution increased while the cut-off magnitude decreased in the later part of each episode. The 2D PCA model of slow earthquakes (Ide & Yabe, 2019) allowed us to interpret the observed changes in the tremor size distribution qualitatively by a decrease in the probability of slip ignition on the fault or an increase in energy dissipation during slip. These changes can be attributed to the release of accumulated stress by slow earthquakes or spatial-temporal variations of pore-fluid pressures during slow earthquakes.

Acknowledgments, Samples, and Data

This study was supported by KAKENHI Grants JP16H06477 (to M. N.), JP19K04050 (to M. N.), and JP18K13639 (to S. Y.) from the Japan Society for the Promotion of Science. All figures were drawn with Generic Mapping Tools (Wessel & Smith, 1998). Seismic waveform data from DONET can be downloaded from http://www.hinet.bosai.go.jp/?LANG=en (National Research Institute for Earth Science and Disaster Resilience, 2019). The earthquake catalog of the Japan Meteorological Agency can be downloaded from http://www.data.jma.go.jp/svd/eqev/data/bulletin/hypo.html. The earthquake catalog of the United States Geological Survey can be downloaded from https://earthquake.usgs.gov/earthquakes/search/.

References

Araki, E., Saffer, D.M., Kopf, A.J., Wallace, L.M., Kimura, T., Machida, Y., Ide, S., Davis, E., & IODP Expedition 365 shipboard scientists (2017). Recurring and triggered slow-slip events near the trench at the Nankai Trough subduction megathrust. Science, 356 (6343), 1157-1160. http://doi.org/10.1126/science.aan3120

Baba, S., Takemura, S., Obara, K., & Noda, A. (2020). Slow earthquakes illuminating interplate coupling heterogeneities in subduction zones. Geophysical Research Letters, 47, e2020GL088089. https://doi.org/10.1029/2020GL088089

Benoit, J., & McNutt, S. (2003). Duration-amplitude distribution of volcanic tremor. Journal of Geophysical Research, 108, 2146. https://doi.org/10.1029/2001JB001520

Bostock, M. G., Thomas, A. M., Savard, G., Chuang, L., & Rubin, A. M. (2015). Magnitudes and moment-duration scaling of low-frequency earthquakes beneath southern Vancouver Island. Journal of Geophysical Research: Solid Earth, 120, 6329–6350. https://doi.org/10.1002/2015JB012195

Chestler, S. R., & Creager K. C. (2017). Evidence for a scale-limited low-frequency earthquake source process. Journal of Geophysical Research: Solid Earth, 122, 3099–3114, https://doi.org/10.1002/2016JB013717

Gao, X., & Wang, K. (2017). Rheological separation of the megathrust seismogenic zone and episodic tremor and slip, Nature, 543, 416–419, https://doi.org/10.1038/nature21389

Gosselin, J. M., Audet, P., Estève, C., McLellan, M., Mosher, S. G., & Schaeffer, A. J., (2020). Seismic evidence for megathrust fault-valve behavior during episodic tremor and slip, Science Advances, 6, eaay5174, https://doi.org/10.1126/sciadv.aay5174

Gutenberg, B., & Richter, C. F. (1944). Frequency of earthquakes in California. Bulletin of Seismological Society of America, 34, 185–188.

Ide, S. (2008). A Brownian walk model for slow earthquakes. Geophysical Research Letters, 35, L17301, https://doi.org/10.1029/2008GL034821

Ide, S. (2010). Striations, duration, migration and tidal response in deep tremor. Nature, 466, 356–359, https://doi.org/10.1038/nature09251

Ide, S., Beroza, G. C., Shelly, D. R., & Uchide, T. (2007). A scaling law for slow earthquakes, Nature, 447, 76–79, https://doi.org/10.1038/nature05780

Ide, S., & Tanaka, Y. (2014). Controls on plate motion by oscillating tidal stress: Evidence from deep tremors in western Japan, Geophysical Research Letters, 41, 3842–3850, https://doi.org/10.1002/2014GL060035

Ide, S., & Yabe, S. (2014). Universality of slow earthquakes in the very low frequency band, Geophysical Research Letters, 41, 2786–2793. https://doi.org/doi:10.1002/2014GL059712

Ide, S., & Yabe, S. (2019). Two-Dimensional Probabilistic Cell Automaton Model for Broadband Slow Earthquakes. Pure and Applied Geophysics, 176, 1021–1036, https://doi.org/10.1007/s00024-018-1976-9

Ikari, M. J., Saffer, D. M., & Marone, C. (2007). Effect of hydration state on the frictional properties of montmorillonite-based fault gouge, Journal of Geophysical Research: Solid Earth, 112, B06423, https://doi.org/10.1029/2006JB004748

Ishimoto, M., & Iida, K. (1939). Observations of earthquakes registered with the microseismograph constructed recently. Bulletin of Earthquake Research Institute University of Tokyo, 17, 443–478.

Ito, Y., Obara, K., Shiomi, K., Sekine, S., & Hirose, H. (2007). Slow Earthquakes Coincident with Episodic Tremors and Slow Slip Events. Science, 315, 503-506. https://doi.org/10.1126/science.1134454

Ito, Y., Obara, K., Matsuzawa, T., & Maeda, T. (2009). Very low frequency earthquakes related to small asperities on the plate boundary interface at the locked to aseismic transition, Journal of Geophysical Research: Solid Earth, 114, B00A13. https://doi.org/10.1029/2008JB006036

Kagan, Y. Y. (2002). Seismic moment distribution revisited: I. Statistical results. Geophysical Journal International, 148, 520–541.

Kaneda, Y., Kawaguchi, K., Araki, E., Matsumoto, H., Nakamura, T., Kamiya, S., Ariyoshi, K., Hori, T., Baba, T., & Takahashi, N. (2015). Development and application of an advanced ocean floor network system for megathrust earthquakes and tsunamis. In Favali P et al. (eds) Seafloor Observatories. Springer, Heidelberg, pp 643–662. https://doi.org/10.1007/978-3-642-11374-1_252

Kaneko, L., Ide, S., & Nakano, M. (2018). Slow earthquakes in the microseism frequency band (0.1–1.0 Hz) off Kii Peninsula, Japan. Geophysical Research Letters, 45, 2618–2624. https://doi.org/10.1002/2017GL076773

Kano, M., Kato, A., & Obara, K. (2019). Episodic tremor and slip silently invades strongly locked megathrust in the Nankai Trough, Scientific Reports, 9, 9270. https://doi.org/10.1038/s41598-019-45781-0

Kao, H., Wang, K., Dragert, H., Kao, J. Y., & Rogers, G. (2010). Estimating seismic moment magnitude (Mw) of tremor bursts in northern Cascadia: Implications for the "seismic efficiency" of episodic tremor and slip. Geophysical Research Letters, 37, L19306. https://doi.org/10.1029/2010GL044927

Kato, A., Iidaka, T., Ikuta, R., Yoshida, Y., Katsumata, K., Iwasaki, T., Sakai, S., Thurber, C., Tsumura, N., Yamaoka, K., Watanabe, T., Kunitomo, T., Yamazaki, F., Okubo, M., Suzuki, S., & Hirata, N. (2010). Variations of fluid pressure within the subducting oceanic crust and slow earthquakes, Geophysical Research Letters, 37, L14310. https://doi.org/doi:10.1029/2010GL043723

Kawaguchi, K., Kaneko, S., Nishida, T., & Komine, T. (2015). Construction of the DONET real-time seafloor observatory for earthquakes and tsunami monitoring, In Favali P et al. (eds) Seafloor Observatories. Springer, Heidelberg, pp. 211–228. https://doi.org/10.1007/978-3-642-11374-1_10

Kitajima, H., & Saffer, D. M. (2012). Elevated pore pressure and anomalously low stress in regions of low frequency earthquakes along the Nankai Trough subduction megathrust, Geophysical Research Letters, 39, L23301. https://doi.org/10.1029/2012GL053793

Liu, Y., & Rice, J. R. (2007). Spontaneous and triggered aseismic deformation transients in a subduction fault model, Journal of Geophysical Research, 112, B09404. https://doi.org/10.1029/2007JB004930

Masuda, K., Ide, S., Ohta, K., & Matsuzawa, T. (2020). Bridging the gap between low-frequency and very-low-frequency earthquakes, Earth Planets and Space, 72:47. https://doi.org/10.1186/s40623-020-01172-8

Matsuzawa, T., Hirose, H., Shibazaki, B., & Obara, K. (2010). Modeling short– and long–term slow slip events in the seismic cycles of large subduction earthquakes, Journal of Geophysical Research, 115, B12301. https://doi.org/10.1029/2010JB007566

Nakajima, J., & Uchida, N. (2018). Repeated drainage from megathrusts during episodic slow slip, Nature Geoscience, 11, 351–356. https://doi.org/10.1038/s41561-018-0090-z

Nakamura, M., & Sunagawa, N. (2015). Activation of very low frequency earthquakes by slow slip events in the Ryukyu Trench. Geophysical Research Letters, 42, 1076–1082. https://doi.org/10.1002/2014GL062929

Nakano, M., Hori, T., Araki, E., Kodaira, S., & Ide, S. (2018). Shallow very-low-frequency earthquakes accompany slow slip events in the Nankai subduction zone. Nature Communications, 9, 984. https://doi.org/10.1038/s41467-018-03431-5

Nakano, M., Yabe, S., Sugioka, H., Shinohara, M., & Ide, S. (2019). Event size distribution of shallow tectonic tremor in the Nankai trough. Geophysical Research Letters, 46, 5828–5836. https://doi.org/10.1029/2019GL083029

National Research Institute for Earth Science and Disaster Resilience (2019), NIED DONET, National Research Institute for Earth Science and Disaster Resilience, https://doi.org/10.17598/NIED.0008

Nishikawa, T., Matsuzawa, T., Ohta, K., Uchida, N., Nishimura, T., & Ide, S. (2019). The slow earthquake spectrum in the Japan Trench illuminated by the S-net seafloor observatories. Science 365 (6455), 808-813. https://doi.org/10.1126/science.aax5618

Nishimura, T., Yokota, Y., Tadokoro, K., & Ochi, T. (2018). Strain partitioning and interplate coupling along the northern margin of the Philippine Sea plate, estimated from Global Navigation Satellite System and Global Positioning System-Acoustic data. Geosphere, 14, 535–551. https://doi.org/10.1130/GES01529.1

Noda, A., Saito, T., & Fukuyama, E. (2018). Slip-deficit rate distribution along the Nankai trough, Southwest Japan, with elastic lithosphere and viscoelastic asthenosphere. Journal of Geophysical Research, 123, 8125–8142. https://doi.org/10.1029/2018JB015515

Obara, K. (2002). Nonvolcanic Deep Tremor Associated with Subduction in Southwest Japan. Science, 296, 1679-1681. https://doi.org/10.1126/science.1070378

Obara, K., Hirose, H., Yamamizu, F., & Kasahara, K. (2004). Episodic slow slip events accompanied by non-volcanic tremors in southwest Japan subduction zone, Geophysical Research Letters, 31, L23602. https://doi.org/10.1029/2004GL020848

Obara, K., & Hirose, H. (2006). Non-volcanic deep low-frequency tremors accompanying slow slips in the southwest Japan subduction zone, Tectonophysics, 417, 33–51. https://doi.org/10.1016/j.tecto.2005.04.013

Obara, K., Tanaka, S., Maeda, T., & Matsuzawa, T. (2010). Depth-dependent activity of non-volcanic tremor in southwest Japan, Geophysical Research Letters, 37, L13306. https://doi.org/10.1029/2010GL043679

Obara, K., & Kato, A. (2016). Connecting slow earthquakes to huge earthquakes. Science, 353, 253-257. https://doi.org/10.1126/science.aaf1512

Rogers, T., & Dragert, H. (2003). Episodic tremor and slip on the Cascadia subduction zone: The chatter of silent slip, Science, 300 (5627), 1942–1943. https://doi.org/10.1126/science.1084783

Scholz, C. H. (1968). The frequency–magnitude relation of microfracturing in rock and its relation to earthquakes. Bulletin of the Seismological Society of America, 58, 399–415.

Scholz, C. H. (2015). On the stress dependence of the earthquake b value. Geophysical Research Letters, 42, 1399–1402. https://doi.org/10.1002/2014GL062863

Staudenmaier, N., Tormann, T., Edwards, B., Mignan, A., & Wiemer, S. (2019). The frequency-size scaling of non-volcanic tremors beneath the San Andreas Fault at Parkfield: Possible implications for seismic energy release, Earth and Planetary Science Letters, 516, 77–107. https://doi.org/10.1016/j.epsl.2019.04.006

Sugioka, H., Okamoto, T., Nakamura, T., Ishihara, Y., Ito, A., Obana, K., Kinoshita, M., Nakahigashi, K., Shinohara, M., & Fukao, Y. (2012). Tsunamigenic potential of the shallow subduction plate boundary inferred from slow seismic slip. Nature Geoscience, 5, 414–418. https://doi.org/10.1038/NGEO1466

Takemura, S., Noda, A., Kubota, T., Asano, Y., Matsuzawa, T., & Shiomi, K. (2019). Migrations and clusters of shallow very low frequency earthquakes in the regions surrounding shear stress accumulation peaks along the Nankai trough. Geophysical Research Letters, 46, 11,830–11,840. https://doi.org/10.1029/2019GL084666

Takemura, S., Yabe, S., & Emoto, K., (2020). Modelling high-frequency seismograms at ocean bottom seismometers: effects of heterogeneous structures on source parameter estimation for small offshore earthquakes and shallow low-frequency tremors, Geophysical Journal International, 223, 1708–1723. https://doi.org/10.1093/gji/ggaa404

Tan, Y. J., & Marsan, D. (2020). Connecting a broad spectrum of transient slip on the San Andreas fault, Science Advances, 6, eabb2489. https://doi.org/10.1126/sciadv.abb2489

Tanaka, S., Matsuzawa, T., & Asano, Y. (2019). Shallow low–frequency tremor in the northern Japan Trench subduction zone. Geophysical Research Letters, 46, 5217–5224. https://doi.org/10.1029/2019GL082817

Tonegawa, T., Araki, E., Kimura, T., Nakamura, T., Nakano, M. & Suzuki, K. (2017). Sporadic low-velocity volumes spatially correlate with shallow very low frequency earthquake clusters. Nature Communications, 8, 2048. https://doi.org/10.1038/s41467-017-02276-8

Warren-Smith, E., Fry, B., Wallace, L., Chon, E., Henrys, S., Sheehan, A., Mochizuki, K., Schwartz, S., Webb, S., & Lebedev, S. (2019). Episodic stress and fluid pressure cycling in subducting oceanic crust during slow slip. Nature Geoscience, 12, 475–481. https://doi.org/10.1038/s41561-019-0367-x

Wech, A. G., Creager, K. C., Houston, H., & Vidale, J. E. (2010). An earthquake-like magnitude-frequency distribution of slow slip in northern Cascadia. Geophysical Research Letters, 37, L22310. https://doi.org/10.1029/2010GL044881

Wessel, P., & Smith, W. H. F. (1998). New, improved version of generic mapping tools released. Eos, Transactions American Geophysical Union, 79(47), 579. https://doi.org/10.1029/98EO00426

Yabe, S., & Ide, S. (2014). Spatial distribution of seismic energy rate of tectonic tremors in subduction zones. Journal of Geophysical Research: Solid Earth, 119, 8171–8185. https://doi.org/10.1002/2014JB011383

Yabe, S., Tonegawa, T., & Nakano, M. (2019). Scaled energy estimation for shallow slow earthquakes. Journal of Geophysical Research: Solid Earth, 124, 1507–1519. https://doi.org/10.1029/2018JB016815

Yabe, S., Baba, S., Tonegawa, T., Nakano, M., & Takemura, S. (2020). Seismic energy radiation and along-strike heterogeneities of shallow tectonic tremors at the Nankai Trough and Japan Trench, EarthArXiv. https://doi.org/10.31223/X57C71

476 Yokota, Y., Ishikawa, T., Watanabe, S., Tashiro, T., & Asada, A. (2016). Seafloor geodetic
477 constrains on interplate coupling of the Nankai Trough megathrust zone. Nature, 534,
478 374–377. https://doi.org/10.1038/nature17632

479 Zal, H. J., Jacobs, K., Savage, M. K., Yarcec, J., Mroczek, S., Graham, K., Todd, E. K., Nakai,
480 J., Iwasaki, Y., Sheehan, A., Mochizuki, K., Wallace, L., Schwartz, S., Webb, S., &
481 Henrys, S. (2020). Temporal and spatial variations in seismic anisotropy and V_P/V_S ratios
482 in a region of slow slip. Earth and Planetary Science Letters, 532, 115970.
483 https://doi.org/10.1016/j.epsl.2019.115970